Study of the optic modes of $Ge_{0.30}S_{0.70}$ glass by infrared and Raman spectroscopy

G. Lucovsky
Xerox Palo Alto Research Center, Palo Alto, California 94304

J. P. deNeufville
Energy Conversion Devices, Troy, Michigan 48084

F. L. Galeener
Xerox Palo Alto Research Center, Palo Alto, California 94304

(Received 18 June 1973; revised manuscript received 10 October 1973)

A study of the room-temperature infrared reflectance and Raman spectra has been made on a $Ge_{0.30}S_{0.70}$ glass. The dominant features of the two spectra are complementary with respect to frequency, and can be understood in terms of a molecular model in which the Ge atoms are fourfold coordinated and S atoms twofold coordinated; the molecular structure in the model is a GeS_4 tetrahedron. Splittings of the bond-stretching modes into two components provide a measure of the intermolecular coupling. Density-of-states effects are clearly present in the low-frequency portions of the spectra, particularly in the Raman spectrum where the bond-bending optic modes and acoustic modes contribute to a continuum of scattering.

I. INTRODUCTION

In crystalline solids, infrared (IR) and Raman activity of optic phonons are determined by selection rules and only a small number of zone-center modes contribute to the first-order spectra. In the transition to an amorphous phase, all of the vibrational modes can become both IR and Raman active due to a disorder-induced breakdown of crystalline selection rules.[1,2] The IR and Raman spectra of an amorphous solid are then expected to display features associated with structure in the one-phonon density of states, as well as matrix-element effects determined by the local order. The essential problem in understanding phonon spectra is therefore analogous to that encountered in electronic spectra: a separation of density-of-states effects from matrix-element effects and a quantitative description of both. This problem is beyond current theoretical capabilities, except perhaps for a-Si and a-Ge, so that it is useful to obtain a qualitative or at best a semiquantitative understanding of the spectra in terms of simple models.

The literature emphasizes differences in the phonon spectra of two important and representative classes of amorphous semiconductors, which in turn have been discussed in terms of two different models. In the first class of amorphous solids, the tetrahedrally coordinated amorphous semiconductors examplified by a-Si, the IR and Raman spectra display similar gross features which have been associated with structure in a one-phonon density of states.[3,4] Differences between the IR and Raman spectra have been attributed to matrix-element effects[5,6]; these however, vary slowly with frequency so that the spectra are still predominantly a reflection of the density of phonon states. In contrast, the IR and Raman spectra of the amorphous chalcogenides, exemplified by a-As_2S_3 show sharper molecularlike spectra in which the IR and Raman activities are frequently complementary.[7-9] The dominant features of these spectra have been explained in terms of a molecular model in which the "molecule" is identified by the differences in coordination between the As (threefold) and S (twofold) atomic sites. The molecule for a-As_2S_3 is the pyramidal structure AsS_3 which has four optic modes, two predominantly bond-stretching modes and two lower-frequency predominantly bond-bending modes. Two bond-stretching modes are observed in the IR and Raman spectra, their relative frequencies and their complementary activity are in accord with the predictions of the molecular model. The two bond-bending modes are not resolved in either the IR or Raman spectrum; moreover, in the Raman spectrum it is impossible to separate out bond-bending optic modes from a continuum of modes extending to very low frequencies and including acoustic modes as well. The inability to resolve the bond-bending modes is a shortcoming of the molecular model and is associated with intermolecular effects. For the lower-frequency modes, both optic and acoustic, a complete description requires the recognition that molecular units, as we have defined them, are interconnected into networks with longer-range order of varying dimensionalities, e.g., the longer-range order is expected to be two dimensional in a-As_2S_3, whereas it is fully three dimensional in a-GeS_2.

In this paper, we present a study of the IR and Raman spectra of a-$Ge_{0.3}S_{0.7}$, an alloy very close

to the compound composition a-GeS_2. We find spectra that are qualitatively similar to those previously reported for a-As_2S_3 and that can be understood in terms of a structural model which contains fourfold coordinated Ge atoms and twofold coordinated S atoms. The high-frequency bond-stretching modes are described by a molecular model in which the molecule is a tetrahedral structure GeS_4. However, there is evidence of intermolecular effects in these modes, e.g., a small splitting of each of the bond-stretching modes into two spectroscopically resolvable components. These intermolecular effects are anticipated to be stronger in a-GeS_2 as opposed to a-As_2S_3 on the basis of the dimensionality argument that was advanced earlier in the paper.

Section II of this paper treats the experimental details relating to sample preparation, compositional characterization, and IR and Raman spectroscopy. Section III presents the experimental results and includes the procedures used for data reduction and analysis. Section IV is a discussion section which includes an interpretation of the spectrum as well as a comparison of this material with other previously studied amorphous semiconductors.

II. EXPERIMENTAL PROCEDURES

A. Sample preparation and characterization

22 g of $Ge_{0.30}S_{0.70}$ were weighed out in a dry N_2 atmosphere using 100-mesh crushed Ge and powdered S, both of 99.999% purity. The ampoule was heated in a rocking furnace as follows:

25–750 °C at 1 °C/min;

750 °C for 18 h;

750–800 °C at 0.5 °C/min;

800–850 °C at 0.25 °C/min;

850–900 °C at 1 °C/min;

900–25 °C at ~200 °C/min (air cooled).

This complex heating schedule was employed to assure that the chemical reaction between the elemental components could occur at a sufficiently low temperature (~750 °C) so that the sulfur vapor pressure could be contained by the fused-silica ampoule until the reaction was complete. At 900 °C the liquid was relatively fluid and completely homogeneous. The vapor pressure at this temperature was relatively high, and a few mg of both S and GeS condensed as crystalline phases during cooling. The maximum deviation of ingot composition which could arise from this vapor condensation is estimated to be ±0.3-at.% Ge and ±0.7-at.% S. The glass obtained by this procedure contained no crystallites as indicated by x-ray diffraction and optical microscopy. The optical quality was good, with few bubbles, no visible inclusions, and relatively uniform refractive index.

B. Infrared measurements

Infrared-reflectivity measurements were made with the sample at room temperature using a Perkin Elmer model-180 spectrometer operated in a double-beam mode. For the spectral range from 800 to 500 cm^{-1}, the detector was a thermopile and the source, a glo bar. In a partially overlapping spectral range from 520 to 60 cm^{-1} the detector was a pyroelectric cell; two sources were used in this spectral range; a glo bar to 100 cm^{-1} and a Hg arc from 120 to 60 cm^{-1}. Reflectance spectra were normalized by comparison with a front-surfaced Al mirror.

C. Raman studies

The Raman scattering measurements were made at room temperature, using an argon-ion laser, Spex double monochromator, RCA C31034 (GaAs) photomultiplier, and photon-counting electronics. The samples were largely transparent to 514.5-nm Ar^+ laser radiation, hence the experiments were carried out at this wavelength in the 90° scattering geometry.

Some sample deterioration was observed. For example, the Raman signal decreased by about 3% per minute when the excitation of 50 mW was focused into a 0.1-mm-diameter beam inside the sample. High-resolution (4 cm^{-1}) scans were accomplished in 10-min periods under these conditions. Sample deterioration during the spectral scan time was eliminated, and the signal-to-noise ratio was improved, by defocusing the 50-mW beam to 0.5-mm diameter and opening the monochromator slits accordingly. Although this procedure forced lower resolution (20 cm^{-1}), comparison with the 4-cm^{-1} scans showed that no significant details were lost. Depolarization spectra computed from both types of scans were indistinguishable. The low-noise depolarization curve reported in this paper was obtained point by point in a manner which minimized exposure of the sample to the defocused beam. The deterioration associated with the focused beam appeared to be permanent, invisible, and confined to the directly irradiated region. The sample was therefore "renewed" by translating it a few hundred microns perpendicular to the laser-beam direction.

The monochromator was equipped with a polarization scrambler. Measurements showed that the resultant instrumental transfer function was the same for both polarizations, and varied linearly by only 7% over the spectral range of the experiments. The spectral curves were not corrected

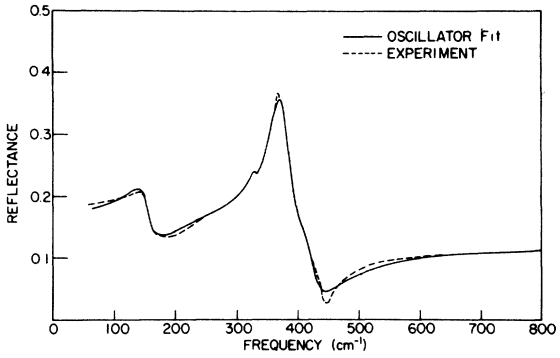

FIG. 1. Room-temperature reflectance spectrum of $Ge_{0.30}S_{0.70}$. The dashed curve is the experimental data; the solid curve the oscillator fit.

for this small variation and, of course, the depolarization curve needed no correction.

III. EXPERIMENTAL RESULTS AND DATA ANALYSIS

The dashed curve in Fig. 1 is the reflectance spectrum of a-$Ge_{0.30}S_{0.70}$ in the spectral range from 800 to 60 cm^{-1}. The important structures consist of a minimum in the reflectivity at approximately 450 cm^{-1}, a shoulder at about 410 cm^{-1}, a peak at 360 cm^{-1}, a weaker peak at 330 cm^{-1}, and finally an edge at about 150 cm^{-1}; these features can be attributed to at most four oscillators. The solid curve is a Lorentzian oscillator fit to the spectrum accomplished by an iterative search in a multiparameter space.[10] Table I contains the oscillator fit parameters; these include a strength S_i, a frequency ν_i^{TO} (in cm^{-1}) and a damping constant Γ_i for each of the four oscillators as well as a high-frequency diclectric constant ϵ_{op}. The dispersion in the complex dielectric constant is then given by

$$\epsilon = \epsilon_{op} + \sum_{i=1}^{4} \frac{S_i(\nu_i^{TO})^2}{(\nu_i^{TO})^2 - \nu^2 - i\Gamma_i\nu\nu_i^{TO}}. \quad (1)$$

One can also calculate a longitudinal frequency ν^{LO} that is associated with each mode. These frequencies are obtained from the maxima in the energy-loss function, $-\mathrm{Im}(1/\epsilon)$ and are tabulated in Table I. Figure 2 contains a plot of the $\nu^2\epsilon_2$, the effective density of states, that is derived from the oscillator analysis.

Figure 3 contains the Raman spectra for the HH and HV polarization configurations. In the HH configuration the polarization vectors of the incident and scattered light are parallel, whereas in the HV configuration they are at right angles. The dominant features of the spectrum are a weak peak at 485 cm^{-1}, a stronger peak at 435 cm^{-1}, and a very strong peak at 342 cm^{-1}. In addition, there is a continuum of scattering between 342 and 435 cm^{-1}, with peaks at 385 and 405 cm^{-1} in the HV spectrum. At lower frequencies, there is scattering at all frequencies below about 250 cm^{-1}. There is weak, but resolvable structure at 200 cm^{-1} (HH), 150 cm^{-1} (HV), 110 cm^{-1} (HV), and 105 cm^{-1} (HH). Kobliska and Solin[9] have demonstrated that the depolarization spectrum, i.e., the ratio of scattering in the HV and HH configurations, S_{HV}/S_{HH} is important in discriminating between structural models. This spectrum is also included in Fig. 3.

Included in Fig. 2 is the reduction of the HH Raman spectrum using the method of Shuker and Gammon.[11] A comparison of this effective density of states ρ_{RS} with the infrared density of states $\nu^2\epsilon_2$ indicates that the dominant features of the two spectra are complementary inasmuch as the dominant feature occurs at different frequencies in the two spectra, 342 cm^{-1} in the Raman spectrum and 367 cm^{-1} in the infrared. A similar type of complementarity has been reported for a-As_2S_3[8,9] wherein the dominant infrared mode is at 309 cm^{-1} and the dominant Raman mode is at 344 cm^{-1}.

IV. DISCUSSION

The first-order IR and Raman spectra of an amorphous semiconductor are expected to reflect structure in the one-phonon density of states, as well as matrix-element effects. A quantitative description of both density-of-states and matrix-element effects is beyond current theoretical capabil-

TABLE I. Oscillator fit parameters for the IR reflectance spectrum of $Ge_{0.30}S_{0.70}$.

Oscillator	Frequency (cm^{-1}) ν_i^{TO}	Strength S_i	Damping constant Γ_i	Longitudinal frequency cm^{-1} ν_i^{LO}
1	409	0.182	0.116	424
2	367	0.758	0.082	
3	328	0.041	0.039	330
4	149	0.708	0.266	158

Optical Frequency Dielectric Constant $\epsilon_{op} = 4.32$

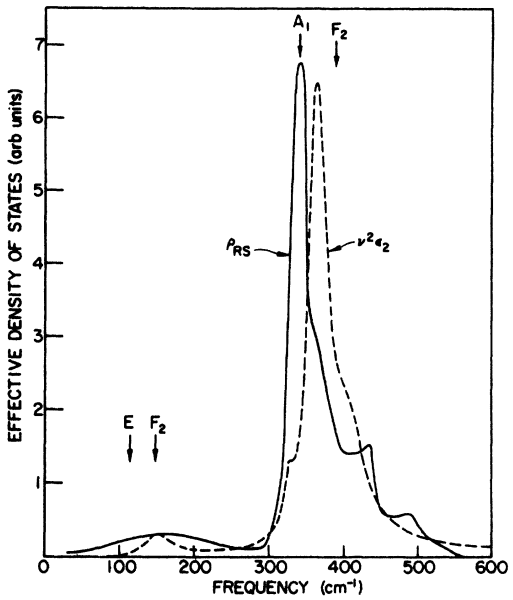

FIG. 2. Infrared and Raman effective density of states for $Ge_{0.30}S_{0.70}$. The infrared density of states $\nu^2\epsilon_2$ is derived from the oscillator fit. The Raman density of states is obtained from the experimental data (HH) using the procedure of Shuker and Gammon (Ref. 11). The frequency markers, A_1, E, F_2, F_2 indicate the modes of a GeS_4 tetrahedral molecule.

ities, except perhaps for a-Si and a-Ge.[5,6] It is therefore useful to apply simple models to more conplex systems such as a-$Ge_{0.3}S_{0.7}$ in order to explain some of the more salient spectral features.

Two different approaches have applied to the IR and Raman spectra of amorphous semiconductors.[12] For a-Si and a-Ge, it has been well established that the reduced IR and Raman spectra are very closely related to the one-phonon density of states.[3,4] Differences in the two spectra (IR and Raman) have been attributed to matrix-element effects which vary only slowly with frequency.[5,6] In contrast, the high frequency and dominant modes of a-As_2S_3 show complementary IR and Raman activity.[8,9] The strong matrix-element (or selection-rule) effect in this material has been emphasized through the application of a molecular model.[7]

The complementary features of the IR and Raman spectra of a-$Ge_{0.3}S_{0.7}$, as shown in Fig. 2, are also the result of strong matrix-element effects and in turn suggest the application of a molecular model. Since the alloy composition we are studying is very close to that of the compound a-GeS_2, we use a structural model that is idealized to the compound composition ($Ge_{0.33}S_{0.67}$). We assume, as was done for a-As_2S_3, that the local coordination satisfies the $8-N$ rule of classical valence-bond chemistry,[13] i.e., that each Ge atom is fourfold coordinated and, at this composition, is bonded only to S atoms, and that each S atom is twofold coordinated and bonded only to Ge atoms. a-GeS_2 is isoelectronic to a-SiO_2, where it is well established that the structural element is an SiO_4 tetrahedron.[14] By analogy the element of local order in a-GeS_2 is a GeS_4 tetrahedron; the tetrahedra are interconnected into a random network through the bridging S atoms.[14] In the molecular approximation we ignore the connected aspect of the amorphous solid and consider the vibrational modes of an isolated tetrahedral molecule.[15]

There are four vibrational modes to consider[15]; two approaches can be used to estimate the frequencies of these optic-type modes. One method is to employ a valence-force-field calculation,[15] wherein the force constants are estimated through the application of an empirically derived relationship.[16-18] A second method, and the one employed in applying molecular models to a-As_2S_3[7-9] and a-As_2S_3,[7,19] is to estimate the frequencies of the "pseudomolecule" of interest from that of a real molecule with a similar structure and similar masses. For example the frequencies for the pyramidal molecule AsS_3 were estimated from those of $AsCl_3$ by using a scale factor obtained from a comparison of the frequencies of the dominant Raman modes.[7,8] In a similar way in Table II we estimate the frequencies of a GeS_4 molecule

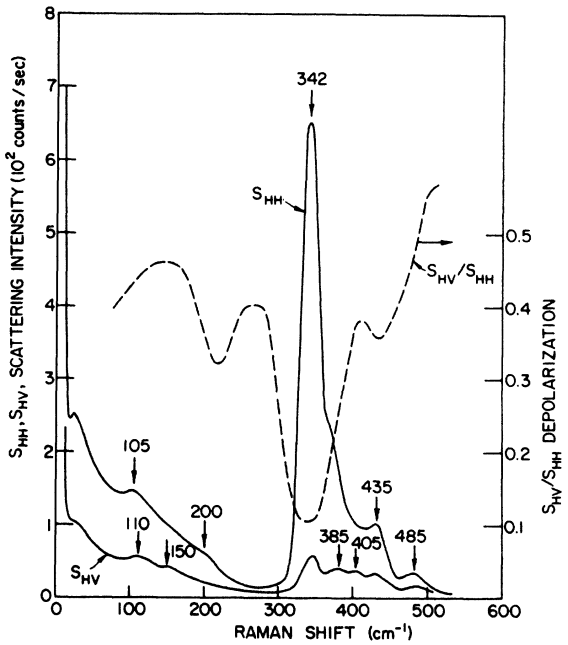

FIG. 3. Room-temperature Raman spectra of $Ge_{0.30}S_{0.70}$. Included in this figure are the HH and HV scattering intensities S_{HH} and S_{HV}, respectively, and the depolarization spectrum S_{HV}/S_{HH}.

TABLE II. Summary of the dominant features of the IR and Raman spectra compared with the frequencies of a GeS_4 molecule.

	IR reflectance		Raman spectrum			GeS_4 molecule	
Mode	Frequency (cm^{-1})	Strength	Frequency (cm^{-1})	Relative intensity (HH)	Depolarization	Frequency (cm^{-1})	Activity
$\nu_1(A_1)$	328	0.041	342	1.00	0.10	342	R
$\nu_2(E)$	...	...	105	0.06	0.43	114	R
$\nu_3(F_2)$	367 409	0.758 0.182	375 (shoulder)	0.34	0.25	388	IR, R
$\nu_4(F_2)$	149	0.708	...	...	...	147	IR, R

from the reported Raman frequencies of the $GeCl_4$ molecule[15]; the scale factor in this comparison is 0.86. In a tetrahedral molecule AB_4, the symmetric Raman mode involves only motion of the four equivalent B atoms[15] and the frequency ω of this mode is given by

$$\omega = (k_r/M_B)^{1/2}, \tag{2}$$

where k_r is the bond stretching force constant and M_B the mass of the B atom. Somayajulu[20] has demonstrated that the bond-stretching force constant $k_r(A,B)$ between two dissimilar atoms (A,B) is related to the bond-stretching force constants of the constituent atoms $[k_r(A,A), k_r(B,B)]$ and their electronegativities (X_A and X_B) by

$$k_r(A,B) = [k_r(A,A)k_r(B,B)]^{1/2} + (X_A - X_B)^2. \tag{3}$$

The ratio of the bond-stretching force constants $k_r(\mathrm{Ge,S})/k_r(\mathrm{Ge,Cl})$ is calculated to be 0.667; taking the relative masses of S and Cl into account, this analysis predicts a frequency ratio $\nu_1(GeS_4)/\nu_1(GeCl_4)$ of 0.858, in excellent agreement with the empirically derived ratio of 0.86. Table II also contains a calculation of the other tetrahedral-molecule frequencies. We first emphasize the two bond-stretching modes, ν_1 and ν_3.

The association of the 342-cm^{-1} feature of the Raman spectrum with the ν_1 mode of the tetrahedral molecule is further supported by its depolarization ratio. The ν_1 mode has A_1 symmetry and is expected to show a strong depolarization; the depolarization spectrum shown in Fig. 3 displays its minimum at 342 cm^{-1} in support of this assignment. In a free AB_4 molecule, the ν_1 mode is only Raman active; however, in a solid, due to intermolecular coupling one anticipates IR activity as well in this mode.[8] We associate the weak feature in the IR reflectance at 328 cm^{-1} with this mode, and in turn assume that the difference in frequency between the IR and Raman frequencies, ~14 cm^{-1}, is a measure of the intermolecular coupling. The strength of the intermolecular force constant can then be estimated from this frequency, and is given by

$$\Delta k = 2(\Delta\omega/\omega)k_r(\mathrm{Ge,S}). \tag{4}$$

$k_r(\mathrm{Ge,S}) \sim 2\times10^5$ dyn/cm, so that $\Delta k \sim 1.8\times10^4$ dyn/cm. In our model, the coupling between molecules is predominantly through forces at the bridging S atoms. These forces are expected to be substantially stronger than the forces between molecules in a true molecular solid wherein the coupling is provided by forces of the van der Waals type.

A similar estimate of the intermolecular coupling is obtained from a comparison of the frequencies of the dominant IR modes with the ν_3 mode of the molecule. The ν_3 mode is an asymmetric stretching mode and is expected to dominate the IR spectrum. We find that there are two oscillators contributing to the dominant IR feature, one at 367 cm^{-1} and one at 405 cm^{-1}. The ν_3 frequency of a GeS_4 molecule is calculated to be 388 cm^{-1}, approximately at the average of these two frequencies. Assuming that the two components we find are the result of intermolecular coupling and applying Eq. (4), we estimate an intermolecular coupling constant of 2.0×10^4 dyn/cm in good agreement with the value obtained from the analysis of the ν_1 mode. Structure in the HV Raman spectrum occurs at 385 and 405 cm^{-1}, whereas a shoulder appears in the HV spectrum at about 375 cm^{-1}. In this interpretation we also associate these features with the ν_3 mode.

In addition to the two bond-stretching modes, an AB_4 molecule has two bond-bending modes, a ν_2 mode of E symmetry which is only Raman active, and ν_4 mode of F_2 symmetry which is both IR and Raman active. As in the case of a-As_2S_3 two modes are not clearly resolved in either the IR or Raman spectrum. In the IR spectrum there is a very heavily damped mode at 149 cm^{-1}, the frequency of the ν_4 mode of a GeS_4 molecule is calculated to 147 cm^{-1}. The HV Raman spectrum also shows a very weak structure at 150 cm^{-1}. The ν_2 mode is anticipated to be only Raman active. There is no evidence for a resolvable second bond-stretching mode in the IR spectrum in the vicinity

of the calculated ν_2 frequency, 114 cm^{-1}; however, there are features at 105 cm^{-1} in the HH Raman spectrum, and at 110 cm^{-1} in the HV spectrum that we assign to the ν_2 mode. However, just as in a-As_2S_3, these features are part of a continuum of scattering that extends from very low frequencies (~ 20–30 cm^{-1}) to just past 200 cm^{-1}. In addition to the features so far assigned to the GeS_4 molecule, and to splittings of molecular modes due to intermolecular coupling, there are also three features in the Raman spectrum that require additional discussion. These are at 200, 435, and 485 cm^{-1}.

Since our alloy a-$Ge_{0.3}S_{0.7}$ is on the S-rich side of the compound GeS_2, it is first tempting to associate these features with S-S vibrations. This type of explanation is reinforced by noting that the S-S stretching modes (as for example reported in the S_8 molecule) are in the vicinity of 475 cm^{-1} and the S bond-bending modes are in the vicinity of 200 cm^{-1}.[21] However, the depolarization spectrum is not in accord with this explanation in as much as an analysis of either ringlike or chainlike S structures yields a symmetric mode at the higher frequency.

In attempts to analyze the spectra of a-As_2S_3 and a-As_2Se_3,[22] there are also additional features that cannot be explained by modes of a pyramidal AsS_3 molecule. These features have been accounted for in terms of a "water-molecule" structure, As-S-As for a-As_2S_3.[7,23] The symmetric character of the feature at 200 cm^{-1} in a-$Ge_{0.3}S_{0.7}$ as evidenced by the local minimum in the depolarization spectrum is in accord with such an explanation, as is the asymmetric character of the modes at 435 and 485 cm^{-1}. However, a quantitative understanding of these additional features requires that the force constants for these modes be different from those estimated for the GeS_4 molecule. At this point it is clear from our work, and that of Kawamoto and Tsuchihashi,[24] who report the 485-cm^{-1} mode over a wide range of compositions including both Ge- and S-rich alloys (with respect to GeS_2), that these additional features are intrinsic modes resulting from the three dimensional network aspect of the structure of this amorphous solid.

V. SUMMARY

We have presented the IR and Raman spectra of a-$Ge_{0.3}S_{0.7}$ and have demonstrated how the dominant features in each spectrum could be explained in terms of a structural model based on a GeS_4 tetrahedron. Effects of intermolecular coupling are clearly observable, as for example splittings of the two high-frequency bond-stretching modes, and other features in the spectrum which were not attributable to modes of a GeS_4 structural unit.

Our analysis of this material emphasizes the importance of considering both density-of-states and selection-rule or matrix-element effects in the spectra of amorphous semiconductors. In the compound amorphous semiconductors, e.g., a-As_2S_3 and a-GeS_2, the high-frequency features can be understood in terms of a molecular model in which these modes are predominantly bond-stretching modes. Both the mode frequencies and their complementary IR and Raman behavior are in accord with this model. Here it is interesting to note that the Raman frequency of an AB_4 tetrahedral molecule is greater than that of the asymmetric IR mode, whereas the reverse is true in a pyramidal AB_3 molecule. Just as it is important to understand the success of the molecular approach, it is equally important to understand and quantify its shortcomings. For example, we have identified a splitting of the two bond-stretching modes with intermolecular coupling and have estimated the magnitude of the coupling force constants. For a-As_2S_3 no such splittings are resolvable. This is consistant with the dimensionality of the network. For a-As_2S_3, the element of order, beyond the local 3-2 coordination, respectively, of the As and S atoms, is two dimensional, whereas in a-GeS_2 it is fully three-dimensional. It is therefore understandable to expect intermolecular coupling to increase as the dimensionality increases and for the spectra to display greater deviation from a molecular model. These deviations from the molecular model are also amenable to a density-of-states description, as for example in a-Si and a-Ge.

It is clear that as experimental data are accumulated and as spectra are better characterized and understood, more sophisticated models will be required. The application of a random-network model to a-Si and a-Ge[5,6] represents the most important step to date in separating out density-of-states and matrix-element effects. More recently, it has been demonstrated by Thorpe[25] that a good density of vibrational states can be developed for a-Si and a-Ge by considering only the local order, i.e., a five-atom tetrahedral structure, and by applying an appropriate potential to the four exterior atoms to describe their interactions with the rest of the amorphous solid. This method is capable of extension to compounds such as a-As_2S_3 and a-GeS_2.

Note added in proof. We have analyzed the reflectance spectrum using a KK analysis and have found that a set of Gaussian oscillators with parameters nearly identical to the present ones provides an improved fit, especially in the vicinity of the reflectivity edge. Details will be published elsewhere.

ACKNOWLEDGMENTS

We wish to acknowledge the assistance of John Tyler in the sample preparation; of William Mosby

and Hugh Six in data acquisition, and of Madeleine Rodoni in the data analysis. We also wish to thank Richard M. Martin for his critical reading of the manuscript.

---

[1]P. G. Dawber and R. J. Elliott, Proc. Phys. Soc. 81, 458 (1963).
[2]P. G. Dawber and R. J. Elliott, Proc. Roy. Soc. Lond. 273, 222 (1963).
[3]J. E. Smith, Jr., M. H. Brodsky, B. L. Crowder, M. I. Nathan, and A. Pinzcuk, Phys. Rev. Lett. 26, 642 (1971).
[4]J. E. Smith, Jr., M. H. Brodsky, B. L. Crowder, and M. I. Nathan, J. Non-Cryst. Solids 8-10, 179 (1972).
[5]R. Alben, J. E. Smith, Jr., M. H. Brodsky and D. Weaire, Phys. Rev. Lett. 30, 1141 (1973).
[6]R. Alben, D. Weaire, J. E. Smith, Jr., and M. H. Brodsky, in Proceedings of The Fifth International Conference on Liquid and Amorphous Semiconductors, Garmisch-Partenkirchen, 1973 (to be published).
[7]G. Lucovsky and R. M. Martin, J. Non-Cryst. Solids 8-10, 185 (1972).
[8]G. Lucovsky, Phys. Rev. B 6, 1480 (1972).
[9]R. J. Kobliska and S. A. Solin, Phys. Rev. B 8, 756 (1973).
[10]H. W. Verleur, J. Opt. Soc. Am. 58, 1356 (1968).
[11]R. Shuker and R. W. Gammon, Phys. Rev. Lett. 25, 222 (1970).
[12]G. Lucovsky, in Ref. 6.
[13]N. F. Mott, Adv. Phys. 16, 49 (1967).
[14]R. J. Bell, N. F. Bird, and P. Dean, J. Phys. C 1, 299 (1968).
[15]G. Herzberg, *Infrared and Raman Spectra of Polyatomic Molecules* (Van-Nostrand, New York, 1945).
[16]R. M. Badger, J. Chem. Phys. 2, 128 (1934); J. Chem. Phys. 3, 710 (1935).
[17]W. Gordy, J. Chem. Phys. 14, 305 (1946).
[18]C. H. Douglas-Clark, Philos. Mag. 18, 459 (1934); Trans. Faraday Soc. 31, 1017 (1935).
[19]I. G. Austin and E. S. Garbett, Philos. Mag. 23, 17 (1971).
[20]S. R. Somayajulu, J. Chem. Phys. 28, 814 (1958).
[21]D. W. Scott, J. P. McCullough, and F. H. Kruse, J. Mol. Spect. 13, 313 (1964).
[22]P. C. Taylor, S. G. Bishop, and D. L. Mitchell, Solid State Commun. 8, 1783 (1970).
[23]E. Finkman, A. P. DeFonzo, and J. Tauc, in Ref. 6.
[24]Y. Kawamoto and S. Tsuchihashi, J. Amer. Ceram. Soc. 54, 131 (1971).
[25]M. F. Thorpe, in Ref. 6.